Emplacement of Lobate Rock-Glacier Landforms and Landscape Modification, Mareotis Fossae, Mars

S. van Gasselt
Freie Universitaet Berlin, Planetary Sciences and Remote Sensing, Malteserstr. 74-100, D-12249 Berlin, Germany
E. Hauber
German Aerospace Center (DLR), Institute of Planetary Research, D-12489 Berlin, Germany
A.P. Rossi
RSSD of ESA. ESTEC, NL 2200 AG, Noordwijk, The Netherlands
G. Neukum
Freie Universitaet Berlin, Planetary Sciences and Remote Sensing, Malteserstr. 74-100, D-12249 Berlin, Germany

Abstract

The so-called fretted terrain at the Martian dichotomy boundary exhibits a variety of creep-related morphologies generally known as lobate debris aprons and lineated valley fills. These features usually occur along troughs and circumferentially to remnant massifs. We here report on investigations of debris aprons and adjacent terrain in the Tempe Terra/Mareotis Fossae region and provide observational evidence for several phases and mechanisms of debris supply at remnant massifs comprising rock fall and large-scale landsliding and terminating with deposition and disintegration of a widespread surficial mantling deposit. The mantling deposit disintegrates by processes similar to thermokarstic degradation as indicated by heavily dissected areas and characteristic shallow and aligned circular depressions. Comparisons of theoretically derived cross-section profiles to topographic measurements along and across lineated-valley fill units, as well as lobate debris aprons, provide additional clues that such creep-related landforms are currently degrading,. It is also shown that a considerable volume of debris/ice is transported along the intra-highland valleys. Such processes might even be active today, as geomorphologic features appear pristine, and crater-size frequency measurements yield ages in the range of 50–100 Ma only. Such observations confirm modeling results of the stability of ground ice on Mars. Various phases of emplacement and degradation confirm theories about cyclic re-deposition of volatiles caused by the changes of the configuration of orbital parameters of Mars.

Keywords: climate; Mars; periglacial; planetary permafrost; rock glaciers.

Introduction

A variety of landforms indicates the possible existence of past or present ice in the near subsurface of Mars (Sharp 1973, Carr 1977 Rossbacher & Judson 1981, Lucchitta 1981). Among the most prominent ice-related features are lobate debris aprons. They have been interpreted to be a mixture of rock particles and ice (Squyres 1978, 1979) analogous to terrestrial rock glaciers, i.e., debris transport systems comprising a mixture of rock fragments and segregational and/or interstitial ice (Barsch 1996). The analogy between terrestrial rock glaciers and Martian lobate debris aprons is mainly based on (a) their lobate shape, (b) the cross-sectional convex-upward profile, (c) characteristic sets of ridges and furrows, and (d) their relationship to adjacent regions indicative of permafrost-related morphologies. Lobate debris aprons have been observed primarily along steep escarpments near the dichotomy boundary (Squyres 1978, 1979, Mangold 2001) and the large impact basin of Hellas Planitia (Squyres 1979, Crown et al. 2002). Rock glaciers are sensitive indicators for the climatic environment during their formation and are thought to be possible large and accessible water reservoirs (Whalley & Azizi 2003). Morphologies of lobate debris aprons in Tempe Terra are similar to terrestrial talus rock glaciers (Whalley 1992, Barsch 1996) which are usually derived from footslope debris situated underneath steep wall-rock of mountainous permafrost environments.

Settings and Observations

The Tempe Terra/Mareotis Fossae region (Fig. 1) is located between 270°E–294°E and 46°N–54°N and is characterized by the steep dichotomy escarpment and the so-called fretted terrain (Sharp 1973) which separates the study area into the southern highland assemblages and a region known as the northern lowland plains. Young surficial deposits interpreted as features related to creep of ice and debris (Squyres 1978, 1979) and mapped as Amazonian surficial units by Scott & Tanaka (1986) fill broad fretted channels of the heavily deformed Noachian highlands, extend from the dichotomy escarpment in northern direction, and are located circumferentially to knobs and remnants of the Noachian basement. The north-south extent of the fretted terrain in our study area varies between 60 km to 170 km. The undissected upland has an elevation of -2700 m at 294°E and about 0 m at 280°E. The lowland has its highest elevations also in the western part of the study area and slopes gently (~0.1°) towards NE, reaching minimum elevations of -4500 m at the eastern border of the study area. Elevation difference between uplands and lowlands decreases from 3000 m to 1500 m.

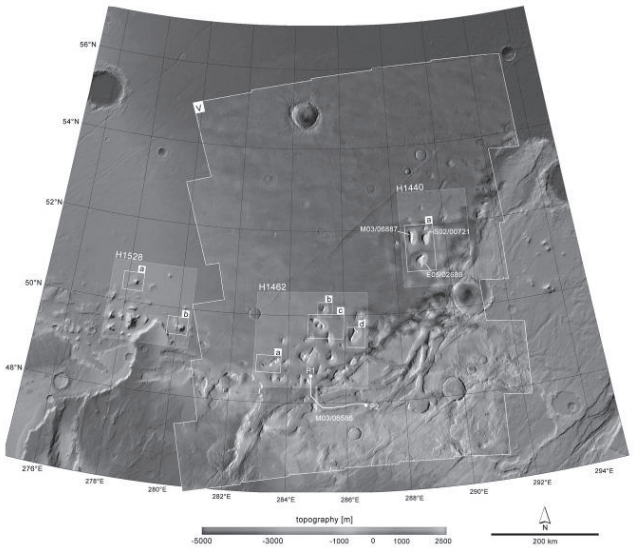

Figure 1. Study area in the Tempe Terra/Mareotis Fossae region as represented by the Viking global image mosaic (MDIM-2.1) superimposed on MOLA (MEGDR) topographic data and location of image scenes discussed in the text; [V] manually processed medium-resolution Viking image mosaic; H1528, H1462, H1440 refer to HRSC image numbers discussed in the text; lettered boxes and white outlines refer to sub-scenes depicted from HRSC image data; individual MOC scenes used in this study are labeled accordingly; P1-P2: topographic profile discussed in the text.

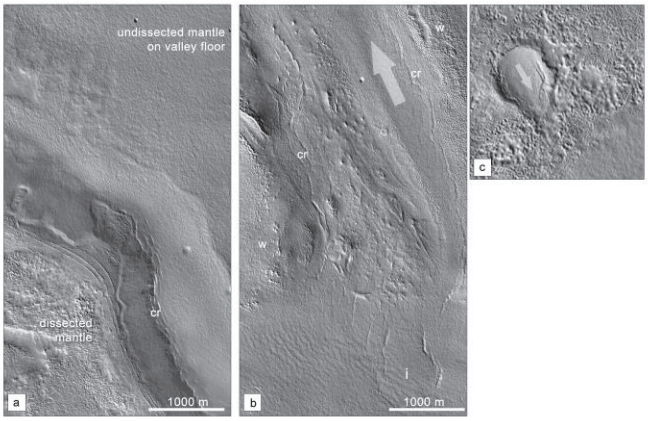

Figure 2. MOC sample scenes of the dichotomy boundary. (a) fretted channel floor (right) and wall (lower left). A mantling deposit is intact on the valley floor, but heavily degraded on the uplands. Crevasses [cr] on the floor of the fretted channels are characteristic of creep and flow of ice and debris. Parallel thin ridges 15–20 m wide run at constant elevations along the upper channel wall. (b) Floor of a fretted channel is covered by a mantling deposit. Crevasses [cr] are situated near the channel walls [w]. They also outline an impact crater completely buried by the mantle [i]. (c) Impact crater filled by mantling deposit. The mantle seems to have flowed out of the crater, scale is 1000 m across.

This difference is slightly less than that reported from the dichotomy boundary on the eastern hemisphere of Mars, i.e., Deuteronilus, Protonilus and Nilosyrtis Mensae, with 2-6 km. Highlands have a generally flat surface, sloping at an angle of less than 0.1° when measured perpendicular to the dichotomy boundary. The surfaces of very large upland segments bounded by fretted channel have larger slopes toward the lowlands (1–2°) and might be tilted as blocks. Such fretted channels have steep walls and flat floors (Squyres 1978), the latter of which are often characterized by so-called "lineated valley fill" (Squyres 1978, 1979}, which is interpreted as material comparable to that of lobate debris aprons but confined to the valley extent. In the study area, fretted valleys have uniform widths of 5–10 km and constant depths of a few hundred meters. The morphologic boundary between highland and lowland areas is characterized by two and sometimes three distinct components: (a) a steep upper slope, i.e., the wall-rock, (b) an intermediate shallow-sloped unit with downslope facing striae, and (c) the highly textured apron (Carr 2001). An intermediate unit is only rarely observed at isolated remnants. At a few sample locations we measured the angles of intermediate units (6°–8°) and angles of debris aprons (2°–4°).

Mantling deposit

A mantling deposit can be observed at scarps and channels near the dichotomy boundary (Fig. 2) as well as around isolated remnant massifs and aprons (Fig. 3) that are located in the lowlands. The deposit does not show any preference to geographical or topographic location, thus, covering all parts of the study area. This observation is based on high-resolution image data (1.5–12 m/pixel) taken with the Mars Orbiter Camera (MOC) that clearly show surfaces at the dichotomy boundary that are covered by that deposit. The mantling deposit is often degraded by erosion, resulting in surfaces whose texture are highly variable, ranging from smooth over stippled, pitted, or knobby to heavily etched. In some places the mantling is completely removed. The disintegration process seems to be controlled by slope aspect, the southern (sun-lit) slopes being more affected than northern slopes.

On the floors of some fretted channels we identify crevasse-like features (Fig. 2). Their specific geometry resembles that of terrestrial chevron crevasses in glaciers, (e.g., Benn & Evans 2003, Menzies 2002). Lineations correspond to longitudinal or transversal lineations and are frequently observed at terrestrial features indicative of creep of ice and debris. Such lineations can be observed at small scales as illustrated in Figure 2. Other lineations are formed by ridges that are thin (15–20 m wide) and extend at approximate constant elevations along upper channel walls; they seem to be genetically connected to the mantling deposit (Fig. 2a). A thick mantling is also observed in a number of image scenes covering the remnant massifs of the Tempe Terra lowland: as seen in Figure 3a, the surface of three debris aprons (A-C) appears relatively smooth although different sets of transversal ridges on the apron can still be observed. The crest of remnant A is characterized by a scalloped and fretted depression (d) and sets of elliptical and aligned shallow depressions on the eastern slope which have a dimension of few tens of meters. Both the crest depression as well as the slope depressions are located in a mantling deposit and

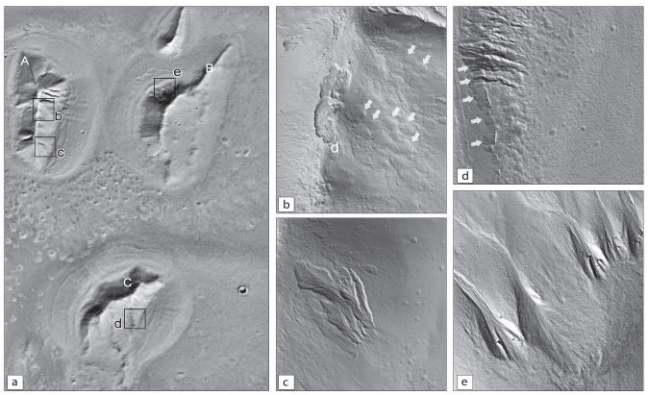

Figure 3. Sample scenes of HRSC in orbit 1440 covering the easternmost study area. Labeled black boxes in (a) refer to MOC sample scenes (b-e). All scenes show indications for the disintegration of a thick mantling deposit. (b) Unusual scalloped depression at remnant crest and elliptical depressions at eastern wall (arrows). (c) Overlapping gullied slide flows. (d) Small slide flows incised into the footslope talus of remnant C. All incision start at the boundary (arrows) between talus and debris apron and are located in a mantling deposit. (e) Slide flows incised into surficial mantling deposit of remnant B.

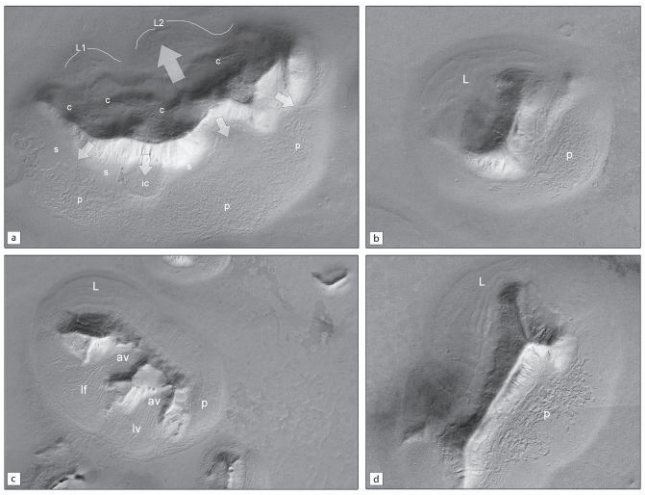

Figure 4. Sample scenes of HRSC in orbit 1462 covering the central lowlands of Tempe Terra. (a) Arcuate remnant massif characterized by an inclined surface tilting towards northern direction; two main directions of transport are observed: large lobes form in northern direction [L1-L2], large coherent debris masses with a pitted surface [p] advance in southern direction. An impact crater [ic] has been completely filled by erosional debris. The talus shows a generally smooth surface texture [s]. Arcuate and sub-parallel furrows on remnant indicate extensional flow [c]. (b) Small isolated remnant knob located northeast of remnant shown in (c); northern apron texture is characterized by ridges and furrows [L], southern apron has a pitted appearance [p]. (c) Alcoves [ac] are incised into remnant massif forming Accumulation zones of debris that is subsequently transported downslope as seen in longitudinal surface lineations. (d) Elongated remnant massif with well-defined crest exhibits transversal ridges and furrows [L] on northern apron and a pitted surface [p] on southern apron. Note also, all aprons are comparable in size when related to the remnant massif.

are indicative of material removal. Mantling-related mass-wasting features are shown in 3c–e where gullied slide flows initiate instantaneously somewhere at the mid-slope, overlap partly and produce faint terminal depositional fans (Fig. 3c, d) that are indicative of dry mass-wasting processes.

As seen in Figure 3d, gullied slide flows can be related to a boundary where the remnant talus abuts the mantling deposit. While the northern sets of slide flows are deeply incised and well expressed, the southern are shallower (Fig 3e).

Disintegration texture

Many debris aprons in Tempe Terra are characterized by surface textures indicative of disintegration of either the surficial mantling deposit or the main debris/ice body. As shown in Figure 4, a slightly northwards inclined and elongated remnant shows a well-pronounced debris apron emerging near the foot of a remnant. While the northern debris apron is characterized by at least two large lobes with transversal ridges (L1–L2), the southern apron is more homogeneously developed with a highly pitted surface texture (p). Below the southern scarp, talus forms as expressed by a relatively smooth texture (s). Eroded remnant material has filled an old impact crater (ic). The southern scarp of the remnant is relatively steep when compared to the northern remnant slope. Flow ridges (c) indicate that material is eroded as coherent sheet and thus contributes to the development of the northern apron. Arrangements of transversal ridges and furrows located on a northern apron and a pitted surface texture located on the southern apron is observed in the scenes depicted in Figures 4b, d. In Figure 4b, the shapes of the remnant massif and debris apron are more circular and the remnant slope angles are approximately comparable in the north and south. However, the northern remnant slopes is composed of a single large bowl-shaped depression in which material is collected from the wall-rock and subsequently transported downslope towards the plains. In Figure 4d, the pitted surface in the south has not reached the terminal area of the apron but is restricted to the remnant footslope. Figure 4c shows well-expressed alcoves (av) at the southwestern remnant slopes and longitudinal sets of furrows and ridges (lf, lv) in the direction of maximum slope gradient. The pitted surface texture seen in Figures 4a, b and d is here restricted to a small area of the southeastern debris apron (p) while lobes (L) are again restricted to the northern apron. In the westernmost region of the Tempe Terra study area, remnants and aprons are developed slightly differently when compared to those in the central and easternmost areas. Northern apron slopes show a ridge-and-furrow texture but it extends asymmetrically farther away from its source. Contrasting to this, the remnant in Figures 5b–b′ is heavily dissected by alcoves and cirque-like features. Towards the north, longitudinal and transversal ridges and furrows prevail while towards the south aprons merge with the apron of the dichotomy escarpment and show sets of depressions at various sizes. For few aprons crater-size measurements could be obtained to derive ages (Fig. 6). Elliptical depressions indicate deformation of impact craters after apron emplacement. In order to obtain the last

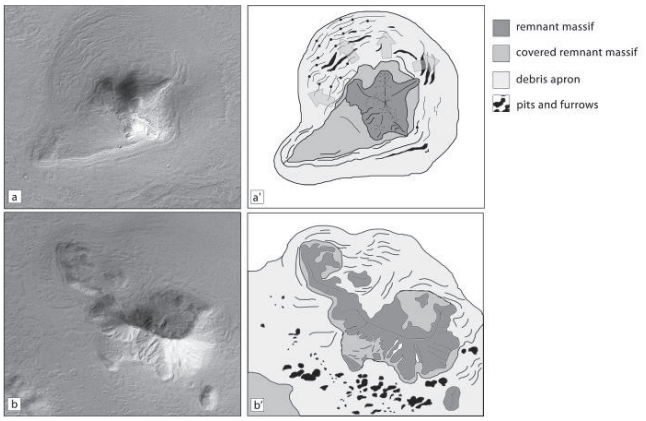

Figure 5. Sample scenes of HRSC in orbit 1528 and schematic maps covering lobate debris aprons of the westernmost study area. Labeled boxes refer to labels in Figure 1; [a–a′] isolated small remnant massif with circumferential lobate debris apron, northern apron shows pattern of ridges and valleys characteristic of compressional flow (ridges) and extensional flow (furrows); [b–b′] flow lineations at debris apron are in longitudinal configuration below alcove depression facing northeast and in transversal configuration under remnant scarp. Southern apron is characterized by pitted texture indicative of degradation.

resurfacing period only fresh-appearing craters have been mapped. Measurements provided ages in the range of 0.01 to 0.05 Ga which is consistent with data obtained from other debris apron (Squyres 1978, Mangold 2003, Berman et al. 2003, Head 2005, Li 2005, van Gasselt 2007).

Geomorphometry

Lobate debris aprons were digitized using a common GIS environment (Fig. 7). We derived geographic coordinates, topographic elevations, lengths, areas and volumes and made simplifications with respect to the (a) base of the debris apron, which was assumed to be horizontal and flat (Barsch 1996), and (b) to the volume of that part of the remnant massif located below its visible extent, i.e., covered by apron debris. In plan view, the remnants north of the dichotomy boundary in Tempe Terra have a more or less irregular polygonal shape and a rugged top, in contrast to the more flat-topped mesas of the type locations in Elysium or Arabia Terra (Mangold & Allemand 2001). The cross-sectional shapes of the aprons are convex upward and steepening towards the terminus of the apron (Fig. 8). The length of debris aprons varies between 1.4 km to 6.3 km averaging at ~4.0 km in northern direction and ~3.5 km in southern direction. The average lengths of aprons are significantly less than values provided by Mangold (2001) with 10.8 to 33 km, and also less than those given by Carr (2001) and Colaprete & Jakosky (1998) with 15 km. Thicknesses of (upper) remnant massifs in Tempe Terra range from ~20 m to ~1100 m. The thickness of aprons varies between ~70 m and ~600 m under the assumption of a flat base. Minimum thickness values are lower than those given by Mangold (2001) (276 m) for the Deuteronilus area, maximum values are about the same. Volumes of debris aprons at Tempe Terra range from <10 km³ to ~300 km³ with a mean surface

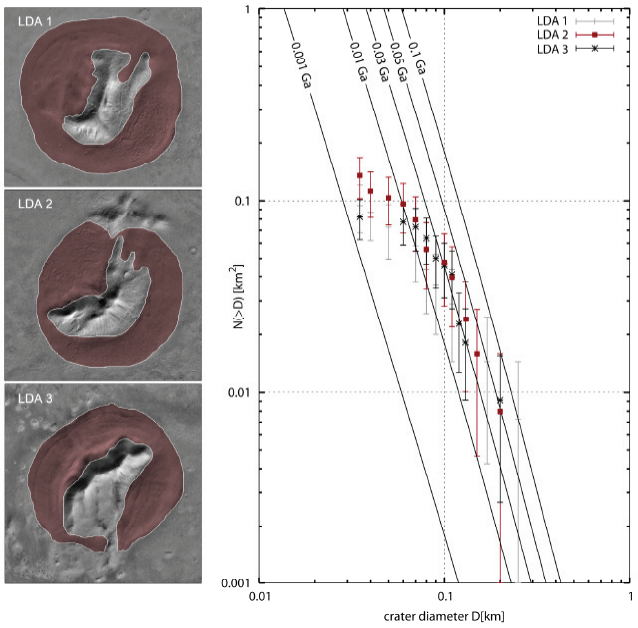

Figure 6. Ages derived for debris-apron surfaces of the central and eastern part of the study area. Stair-stepped distribution indicates multiple episodes of erosional activity, derivation of isochrones (in Ga) are based on Hartmann and Neukum (2001) with the polynomial production function coefficients by Ivanov (2001); for a discussion on errors, see Neukum et al. (2004).

area of ~282 km² (Fig. 7). The remnants have a mean size of ~115 km² (15 to >1000 km²) and a mean volume of ~21 km³ (<5 to 200 km³). As Barsch (1996) summarizes, there might be a close relationship between the source area of debris production and the surface area of a (terrestrial) rock glacier at the footslope with values between 1:1.36 to 1:4.4 (Wahrhaftig & Cox 1959, Barsch 1977, Gorbunov 1983). From 27 observations at Tempe Terra we obtain a factor of 2 for the remnant size when compared to the area occupied by the debris apron. Mangold (2001) calculated the basal shear stress and obtained values in the range of $\sigma = 34–108$ kPa for the Deuteronilus/Protonilus Mensae areas. These values are lower than photoclinometrically derived values by Squyres (1978). For the Tempe Terra region we obtain values between 6.7–82.4 kPa for average apron lengths, with an average of ~38 kPa. The calculated values are not consistent with basal shear stresses given for terrestrial rock glaciers by Whalley (1992) with 100–300 kPa. This may indicate an ice content which is higher (Hauber et al. 2007) than typically considered for rock glaciers or very low strain rates due to a low shear stress. Inactive rock glaciers tend to have generally lower slopes as either debris material was eroded or volatiles were removed, subsequently causing thermokarstic degradation of the rock-glacier surface (Barsch 1996, Ikeda & Matsuoka 2002, Berthling et al. 1998).

Discussion and Conclusions

Image data provide observational evidence for the existence of a widespread mantling deposit in the Tempe Terra/Mareotis Fossae region which covers not only debris

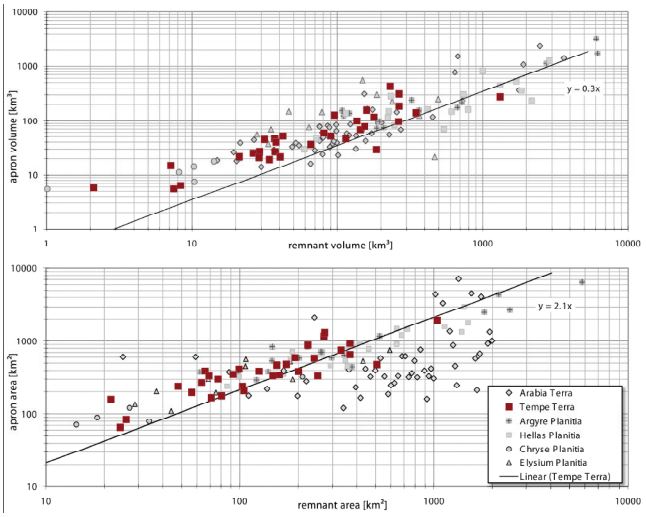

Figure 7. Plot of derived ratios between volumes (a) and areas (b) of remnant massifs and debris aprons as indicator for the degradational state. Values of Tempe Terra massifs and debris aprons (dark squares) are approximated by linear fit.

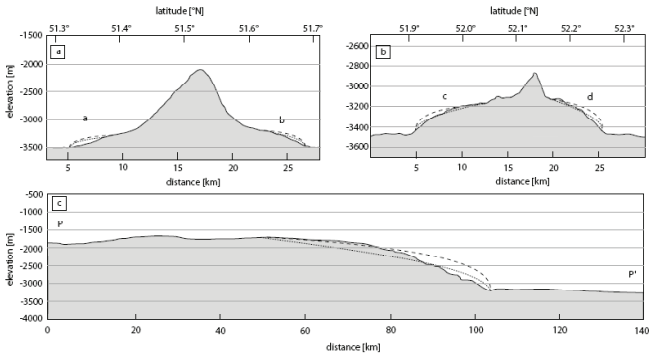

Figure 8. MOLA-based topographic profiles across debris aprons (a, b) and along fretted channel (c) and theoretic profiles of debris aprons obtained from equation derived by Paterson (2001).

aprons of the lowlands but also the escarpment of the Martian dichotomy boundary. At the dichotomy escarpment this mantling deposit shows several characteristics of creep and deformation as well as for processes of disintegration similar to thermokarstic degradation of ice-rich surface materials. Indicators for the mobility of that mantling deposit are found at various locations.

We confirm the presence of a mantle at latitudes higher than ~30–50° as inferred from global-scale roughness maps (Kreslavsky 2000) and directly observed in MOC images (Carr 2001, Malin 2001). Flow lineations on debris aprons resemble closely features known from terrestrial rock glaciers comprising various sets of transversal and longitudinal ridges and furrows indicative of differential movements controlled by subsurface topography. At several locations in Tempe Terra, southward-facing debris aprons show a pitted surface texture that is interpreted as indicators for thermokarstic degeneration and loss of volatiles subsequently leading to collapse and formation of shallow depressions or pits. Their restricted extent suggests control by sun-irradiation (Rossi et al. 2008). Shallow depressions form primarily in mantling material covering remnant massifs whereas pits and furrows are more often observed on the debris-apron surface. Degradation of surfaces is also confirmed by observations of theoretically derived cross-profiles of debris aprons and lineated valley fill units. Both creep-related landforms show an unsatisfactory fit to the model curve. The convex-upward shape of lineated valley fill at the entrance of fretted channels shows not only debris transport perpendicular to valleys walls but also in parallel direction. This furthermore indicates that flow lineations seen in lineated valley fill deposits are not only caused by compression but also by the downslope movement along the valley. It is suggested that the main processes of landsliding and rockfall had come to an end and that subsequent deposition of a mantling deposit caused smoothing of the underlying topography and allowed formation of such slides and gullied flows. Resurfacing ages of 0.01 to 0.05 Ga are consistent with ages obtained from other debris apron locations on Mars. Geomorphometrically derived area ratios of the depositional zone and source area show values that are comparable to estimates given in Barsch (1996) for terrestrial rock glaciers, indicating that the genetic configuration is comparable. Geologically recent degradational and thermokarstic processes are in good agreement with modeling work of obliquity variations of the planet's rotational axis and variations of the planet's eccentricity and precession (Murray et al. 1973, Pollack 1979, Toon et al. 1980, Jakosky et al. 1995). It was shown that prolonged periods of higher obliquity lead to mobilization of volatiles at the poles and to precipitation at lower latitudes (Levrard et al. 2004). This process (a) might have lead to saturation of remnant-related talus deposits with ice causing subsequently creep of debris, and (b) also contributed to a mid-latitudinal mantling deposit (Rossi et al. 2008).

References

Barsch, D. 1977. Eine Abschätzung von Schuttproduktion und Schutttransport im Bereich aktiver Blockgletscher der Schweizer Alpen, Z. *Geomorph. Supp.* 28: 148-–160.

Barsch, D. 1996. *Rockglaciers: indicators for the present and former geoecology on high mountain environments.* Berlin, Germany: Springer, 331 pp.

Benn, D.I. & Evans, D.J.A. 2003. *Glaciers and glaciation*. London, England: Arnold, x+734 pp.

Berman, D.C., Hartmann, W.K. & Crown, D.A. 2003. Debris aprons, channels, and volcanoes in the Reull Vallis region of Mars. In: *Lun. Planet. Sci. Conf. Abs., XXXIV, #1879, 12-17 March.* CD-ROM. League City, Tex., USA: Lun. Planet. Inst.

Berthling, I., Etzelmüller, B., Eiken, T. & Sollid, J.L. 1998. Rock glaciers on Prins Karls Forland, Svalbard. I: internal structure, flow velocity and morphology. *Permafrost Perigl. Proc.* 9(2): 135-145.

Carr, M.H. & Schaber, G.G. 1977. Martian permafrost features. *J. Geophys. Res.* 82(11): 4039-4054.

Colaprete, A. & Jakosky, B.M. 1998. Ice flow and rock glaciers on Mars. *J. Geophys. Res.* 103(E3): 5897-5909.

Crown, D.A., Pierce, T.L., McElfresh, S.B.Z. & Mest, S.C. 2002. Debris aprons in the eastern hellas region of mars: Implications for styles and rates of highland degradation. In: *Lun. Planet. Sci. Conf. Abs., XXXIII, #1642*. CD-ROM. League City, Tex, USA.

Gasselt, van S., Hauber, E. & Neukum, G. 2007. Cold-climate modification of Martian landscapes: A case study of a spatulate debris landform in the Hellas Montes region, Mars. *J. Geophys. Res.* 112 (E09006).

Gorbunov, A. 1983. Rock glaciers of the mountains of middle Asia. *Proceedings of the Fourth International Conference on Permafrost, Fairbanks, Alaska*: 359-362.

Hartmann, W.K. & Neukum, G. 2001. Cratering chronology and the evolution of Mars. *Space Sci. Rev.* 96(1-4): 165-194(30).

Hauber, E., van Gasselt, S., Chapman, M.G. & Neukum, G. 2007. Geomorphic evidence for former lobate debris aprons at low latitudes on Mars: indicators of the Martian paleoclimate. *J. Geophys. Res.* 112: E09006, doi:10.1029/2006JE002842.

Head, J.W., Neukum, G., Jaumann, R. et al. 2005. Tropical to mid-latitude snow and ice accumulation, flow and glaciation on Mars. *Nature* 434: 346-351.

Ikeda, A. & Matsuoka, N. 2002. Degradation of talus-derived rock glaciers in the Upper Engadin, Swiss Alps. *Permafrost Perigl. Proc.*13(2): 145-161.

Ivanov, B.A. 2001. Mars/Moon cratering rate ratio estimates. *Space Sci. Rev.* 96(1-4): 87-104(18).

Jakosky, B.M., Henderson, B.G. & Mellon, M.T. 1995. Chaotic obliquity and the nature of the Martian climate. *J. Geophys. Res.* 100(E1): 1579-1584.

Kreslavsky, M. & Head, J.W. 2000. Kilometer-scale roughness of Mars: results from MOLA data analysis. *J. Geophys. Res.* 105: 26,695-26,712.

Laskar, J., Correia, A.C.M., Gastineau, M., Joutel, F., Levrard, B. & Robutel, P. 2004. Long term evolution and chaotic diffusion of the insolation quantities of Mars. *Icarus* 170(2): 343-364.

Levrard, B., Forget, F., Montmessin, F. & Laskar, J. 2004. Recent ice-rich deposits formed at high latitudes on Mars by sublimation of unstable equatorial ice during low obliquity. *Nature* 431: 1072-1075.

Li, H., Robinson, M.S., & Jurdy, D.M. 2005. Origin of Martian northern hemisphere mid-latitude lobate debris aprons. *Icarus* 176(2): 382-394.

Lucchitta, B.K. 1981. Mars and Earth–comparison of cold-climate features. *Icarus* 45(2): 264-303.

Lucchitta, B.K. 1984. Ice and debris in the fretted terrain, Mars. *J. Geophys. Res.,* Supp. 89(B1): B409-B419.

Mangold, N. 2001. Lobate debris aprons as potential targets for ground ice detection analogs to terrestrial rock glaciers. In: *Conf. Geophys. Detect. Subsurf. Water Mars, #7009.* Houston, Tex., USA: Lun. Planet. Inst.

Mangold, N. & Allemand, P. 2001. Topographic analysis of features related to ice on Mars. *Geophys. Res. Lett.* 28(3): 407-410.

Mangold, N. 2003. Geomorphic analysis of lobate debris aprons on Mars at Mars Orbiter Camera scale: evidence for ice sublimation initiated by fractures. *J. Geophys. Res.* 108(E4): 8021.

Menzies, J. (ed.) 2002. *Modern and Past Glacial Environments.* Oxford, England: Butterworth-Heinemann, xxii+5543 pp.

Milliken, R.E., Mustard, J.F. & Goldsby, D.L. 2003. Viscous flow features on the surface of Mars: observations from high-resolution Mars Orbiter Camera (MOC) images. *J. Geophys. Res.* 108(E6): 5057.

Murray, B.C., Ward, W.R. & Yeung, S.C. 1973. Periodic insolation variations on Mars. *Science* 180(4086): 638-640.

Mustard, J.F., Cooper, C.D. & Rifkin, M.K. 2001. Evidence for recent climate change on Mars from the identification of youthful near-surface ground ice. *Nature* 412: 411–414.

Neukum, G., Jaumann, R., Hoffmann, H. et al. 2004. Recent and episodic volcanic and glacial activity on Mars revealed by the High Resolution Stereo Camera. *Nature*. 432: 971-979.

Paterson, W.B. 2001. *The Physics of Glaciers*, 3rd ed. London, England: Butterworth-Heinemann, ix+496 pp.

Pollack, J.B. 1979. Climatic change on the terrestrial planets Icarus 37(3): 479-553.

Rossbacher, L.A., & Judson, S. 1981. Ground ice on Mars—inventory, distribution, and resulting landforms. *Icarus* 45(1): 39-59.

Rossi, A.P., van Gasselt, S., Pondrelli, M., Zegers, T., Hauber, E. & Neukum, G. 2008. Periglacial landscape evolution at Lower Mid-Latitudes on Mars: The Thaumasia Highlands, *Proceedings of the Ninth International Conference on Permafrost, Fairbanks, Alaska, June 29–July 3, 2008* (this proceedings).

Scott, D.H. & Tanaka, K.L. 1986. *Geologic map of the western equatorial region of Mars*. 1:15,000,000. Map I-1802-A. U.S. Geol. Surv. Misc. Inv. Ser.

Squyres, S.W. 1978. Martian fretted terrain: flow of erosional debris. *Icarus* 34(3). 600-613.

Squyres, S.W. 1979. The distribution of lobate debris aprons and similar flows on Mars. *J. Geophys. Res.* 84(B14): 8087-8096.

Sharp, R.P. 1973. Mars: fretted and chaotic terrains. *J. Geophys. Res.* 78: 4073-4083.

Toon, O.B., Pollack, J.B., Ward, W., Burns, J.A. & Bilski, K. 1980. The astronomical theory of climatic change on Mars. *Icarus* 44(3): 552-607.

Wahrhaftig, A.L. & Cox, A. 1959. Rock glaciers in the Alaska Range. *Bull. Geol. Soc. Am.* 70: 383-436.

Whalley, W. 1992. A rock glacier in South Ellendalen, Lyngen Alps. *Norsk Geografisk Tidsskrift* 46: 29-31.

Whalley, W.B. & Azizi, F. 2003. Rock glaciers and protalus landforms: analogous forms and ice sources on Earth and Mars. *J. Geophys. Res.* 108(E4): 8032.